Acetaldehyde Tosylhydrazone, Sodium Salt. A dispersion of 60% NaH/mineral oil (1 equiv; Aldrich) was added to a stirred solution of the tosylhydrazone (ca. 0.25 g) in 20 mL of CH_2Cl_2. After 1 h, 25 mL of pentane was added, causing the salt to precipitate as a sticky, off-white solid. The salt was collected by suction filtration, washed with cold hexane, and dried in vacuo. The product, obtained in quantitative yield, was crushed to a fine powder and used without further purification.

Diazoethane (1a). The freshly prepared tosylhydrazone salt was placed in a 10-mL round-bottomed flask. A glass adapter arm (essentially a short-path distillation column) connected the flask to a collection tube. The system was evacuated (<1 Torr), and the salt was heated to 40 °C for 30 min with use of a silicone oil bath. Pyrolysis was then effected by raising the temperature to 95 °C for 90 min. The yellow-orange diazoethane condensed in the collection tube, which had been cooled with liquid N_2. The liquid N_2 bath was replaced with a methylcyclohexane slush bath (-126 °C), and the system was vented with dry N_2. After the collection tube was transferred to the matrix isolation apparatus, the sample was subjected to 3 freeze-pump-thaw cycles at -126 °C (the sample was not allowed to warm above ca. -100 °C). After the pressure in the matrix-isolation system had fallen below 5×10^{-6} Torr, diazoethane was sublimed from the -126 °C slush bath and co-deposited with either argon or N_2 on a cold window maintained at 30 or 24 K, respectively. ^{1}H NMR ($CDCl_3$) δ 1.77 (d, 3 H, J = 5.5 Hz), 3.39 (q, 1 H, J = 5.5 Hz);[48] UV (CH_3CN, 298 K) λ_{max} 222, 468 nm;[46,49] UV (Ar, 9 K) λ_{max} 215 nm; IR (Ar, 8 K) 3091 (m), 2989 (w), 2955 (m), 2907 (m), 2866 (w), 2094 (s), 2063 (vs), 1606 (m), 1482 (w), 1462 (w), 1440 (m), 1388 (m), 1092 (w), 900 (m), 852 (w), 581 (m), 454 (m), 418 (m) cm^{-1}.

2,2,2-Trideuterioacetaldehyde was prepared by pyridine-catalyzed exchange of deuterium (from D_2O) for hydrogen in acetaldehyde.[50] ^{1}H NMR showed the product to be 80% acetaldehyde-d_3 and 20% acetaldehyde-d_2 ($CDCl_3$): δ 2.18 (m [1:3:5:5:3:1], 1 H, J = 3 Hz, C*H*D$_2$CHO), 9.80 (br s, 4.8 H, CHD$_2$C*H*O + CD$_3$C*H*O). (A ratio of 1:3:5:5:3:1 requires that $^3J_{H-H} \approx {}^2J_{H-D}$).

2,2,2-Trideuterioacetaldehyde tosylhydrazone was synthesized in 77% yield using the procedure described for the protiated analog. Mp 84-85.5 °C; ^{1}H NMR ($CDCl_3$) δ 2.43 (s, 3 H), 6.87 and 7.19 (both br s, 1 H; syn and anti isomers of hydrazone), 7.32 (dd, 2 H), 7.44 and 7.53 (both s, 1 H; two isomers); 7.84 (dd, 2 H); mass spectrum, m/z (relative intensity) 215 (M$^+$, 0.9), 214 (0.5), 173 (14), 172 (14), 155 (41), 141 (25), 140 (17), 139 (44), 109 (21), 108 (24), 107 (18), 93 (58), 92 (63), 91 (100).

2,2,2-Trideuteriodiazoethane (1b) was prepared using the procedure described for the protiated analog: IR (0.55% CO in Ar, 8 K) 3088 (m), 2216 (m), 2065 (vs), 1947 (m), 1385 (s), 1109 (w), 1058 (w), 547 (m) cm^{-1}.

1-Diazo-2-propanone (6) was prepared from pentane-1,3-dione by diazo transfer reaction with p-carboxybenzenesulfonazide (Aldrich) followed by basic hydrolysis.[51] ^{1}H NMR ($CDCl_3$) δ 2.11 (br s, 3 H), 5.25 (br s, 1 H); IR (Ar, 9 K) 2109 (vs), 2088 (m), 1669 (s) cm^{-1}. The compound was sublimed at -63 °C (<5×10^{-6} Torr) and codeposited with argon to form a matrix.

Note Added in Proof. Diazoethane (**1**) was subjected to the following sequence of photolysis conditions in a methylcyclohexane glass at 4.2 K: $\lambda > 237$ nm (1 h), $\lambda > 399$ nm (2 h), $\lambda = 460 \pm 6.5$ nm (2.4 h). ESR spectra recorded after each irradiation interval reveal no triplet transitions. As in the case of N_2 matrices (vide supra), we conclude either that vibrationally hot ethylidene is not the cause of our inability to observe triplet ethylidene (**3**) or that a methylcyclohexane matrix is ineffective at quenching vibrationally hot ethylidene.

Gallo and Schaefer recently computed a singlet-triplet splitting of 5 ± 1 kcal/mol for ethylidene (**3**) (Gallo, M. M.; Schaefer, H. F., III *J. Phys. Chem.* **1992**, *96*, 1515-1517).

Acknowledgment. We gratefully acknowledge the National Science Foundation for research support (CHE-9003319). R.J.M. is the recipient of an NSF Presidential Young Investigator Award (CHE-8957529), a 3M Nontenured Faculty Grant Award, and a DuPont Young Faculty Grant. We thank Professor M. S. Platz (Ohio State University) for a preprint concerning excited state processes on dialkyldiazirines.

(48) Ledwith, A.; Friedrich, E. C. *J. Chem. Soc.* **1964**, 504-507.
(49) Bradley, J. N.; Cowell, G. W.; Ledwith, A. *J. Chem. Soc.* **1964**, 353-357.
(50) Baldwin, J. E.; Pudussery, R. G. *Chem. Commun.* **1968**, 408.
(51) Hendrickson, J. B.; Wolff, W. A. *J. Org. Chem.* **1968**, *33*, 3610-3618.

Framework Crystal Structure Solution by Simulated Annealing: Test Application to Known Zeolite Structures

Michael W. Deem† and John M. Newsam*

Contribution from Exxon Research and Engineering Company, Route 22 East, Annandale, New Jersey 08801, and BIOSYM Technologies Inc., 9685 Scranton Road, San Diego, California 92121-2777. *Received April 15, 1991*

Abstract: Direct, real-space solution of zeolite framework crystal structures by simulated annealing has been explored as an alternative to conventional powder diffraction or model-building methods. The method, as well as its success in predicting the framework structures of known zeolites, is described in detail. Data taken as input to the method are unit cell dimensions, symmetry, and framework density. The general geometrical characteristics of the 4-connected framework structures of zeolite materials are captured by a figure of merit that contains terms based on T-T distances (T = tetrahedral species, Si or Al etc.), T-T-T angles and average angles, degree of T-atom coordination, appearance of 3-connectedness in projection, and cylindrical or spherical pore size. Test solutions of 64 known zeolite structures with 6 or fewer unique T-atoms give a successful result in 57 cases. Low-symmetry systems, in particular, tend to give rise to large numbers of hypothetical 4-connected structures that satisfy the geometrical considerations, and in total, more than 5000 hypothetical structures have been produced. The observed structure usually ranks among those with the lower values of the figure of merit. Incorporation of a sample-specific contribution to the figure of merit based on the degree to which the model matches a target powder diffraction pattern improves the success of the method. This additional term almost invariably causes the observed, known structure to have the lowest value of the figure of merit, and it is thus a great aid in practical structure solution.

1. Introduction

Structure solution continues to be a taxing aspect of the characterization of crystalline materials that occur only in polycrystalline form (i.e. in which individual crystallite sizes are smaller than some 10 μm). The past decade has seen substantial improvements in both neutron and X-ray diffraction methods, notably in the use of synchrotron X-radiation,[1] but initial solutions of the

* To whom correspondence should be sent at BIOSYM Technologies, Inc.
† Present address: Department of Chemical Engineering, University of California at Berkeley, Berkeley, CA 94720.

(1) Newsam, J. M.; Liang, K. S. *Int. Rev. Phys. Chem.* **1989**, *8*, 289-338.

0002-7863/92/1514-7189$03.00/0

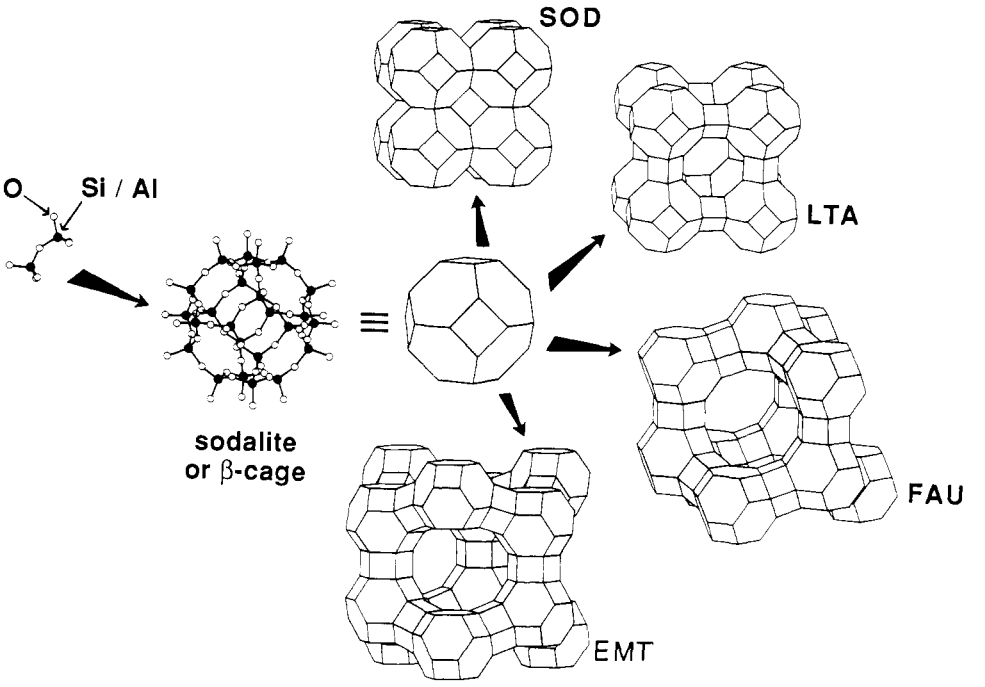

Figure 1. Illustration of the manner of construction of zeolite frameworks from TO_4 tetrahedra. A pair of such tetrahedra sharing one vertex is linked into a sodalite or β cage. In a simpler representation, the oxygen atoms are omitted and the cage is drawn as straight lines connecting adjacent T-sites (with hidden lines removed in this case). It is clear that the framework oxygen atoms lie close to the midpoints of the T–T linkages, reducing the problem of initial framework structure solution to that of determining the T-atom positions. The sodalite cage unit is found in the structures of sodalite (framework code SOD), Linde type A (LTA), faujasite (FAU), ECR-30 and EMC-2 (EMT).

framework structures of materials such as zeolites remain troublesome. Paralleling these advances have been improvements in computational methods that for powder diffraction data facilitate both structure solutions and subsequent refinements. We have recently outlined a new approach to framework structure *solutions* that generates trial models satisfying established geometrical constraints for the class of materials under consideration, subject to the measured unit cell dimensions, symmetry, and composition.[2,3] We describe here extensions of this method and a systematic evaluation of its applicability to zeolites based on attempted "solutions" of 64 of the 85 currently known zeolite framework types. While geometrical constraints alone are sufficient to generate most of these structures successfully, the effectiveness of the method is significantly enhanced on incorporating diffraction data directly into the structure solution procedure. In the majority of cases a function consisting solely of framework density and powder X-ray diffraction (PXD) information proves sufficient for structure solution, underlining that this method can be applied quite generally.

2. Methodology

2.1. Common Structural Features. Zeolites are classically crystalline aluminosilicates with framework structures built from silicate and aluminate tetrahedra[4] (Figure 1). Each apical oxygen atom of the tetrahedron is shared with an adjacent tetrahedron, leading to a framework composition TO_2, where T is the tetrahedral species, Si or Al etc. Geometrically, the midpoints of the T–T vectors are sufficiently close to the actual positions adopted by the apical oxygen atoms to allow least-squares optimization of the coordinates based on distance constraints[5,6] or diffraction pattern matching (e.g. refs 7 and 8). The problem of structure solution for framework structures of this type thus reduces to that of determining initial T-atom positions. Each T-atom is connected to exactly four first neighbor T-atoms and the T-atom bonding requirements define constraints on the possible T–T distances and T–T–T angles. Additionally, zeolite frameworks are, by definition, open with accessible micropore volume that is intrinsic to the crystal structure. The micropore volume and information about the size of the apertures controlling access to this internal pore space are obtained by sorption experiments and by thermogravimetric analyses (tga). An additional characteristic of most observed zeolite frameworks is high intrinsic symmetry (which may be reduced by ordering phenomena or by distortions induced by composition or conditions). Also, most zeolite structures when viewed in projection along one or more directions appear as 3-connected 2-dimensional nets, with neighboring T-atom nodes being not far from equidistant (Figure 2). These general characteristics form the basis of a measure of the reasonableness of a given arrangement of T-atoms. There are, it is to be noted, other features common to certain families of zeolites, such as secondary building units, or the presence of 4-, 5-, 6-, or 8-rings, but these less general characteristics have not been incorporated into the present method.

2.2. General Method of Framework Structure Solution. It is often straightforward to index the powder X-ray diffraction (PXD) pattern measured from a new zeolite material. A successful indexing yields the unit cell dimensions and, based on a judgement of which peaks are systematically absent from the PXD pattern, a choice of a single or, more commonly, a small number of possible space groups. The chemical composition and the sorptive characteristics of the material indicate the framework density or, expressed in another way, the number of tetrahedra that are contained within the measured unit cell. The chemical composition also indicates whether the material has a 4-connected framework (T:O = 0.5) or an interrupted framework in which one or more apical oxygen atoms terminates as a hydroxyl function (T:O < 0.5).

Framework structure solution is then the step of determining approximate positions for these T-atoms within the unit cell. Once approximate positions have been determined, conventional

(2) Deem, M. W.; Newsam, J. M. *Nature* **1989**, *342*, 260–262.
(3) Newsam, J. M.; Deem, M. W. U.S. Patent Appl. No. 356320, 1989.
(4) Newsam, J. M. *Science* **1986**, *231*, 1093–1099.
(5) Meier, W. M.; Villiger, H. Z. *Kristallogr.* **1969**, *129*, 411–423.
(6) Baerlocher, C.; Hepp, A.; Meier, W. M. *DLS-76—A Program for Simulation of Crystal Structures by Geometric Refinement*; ETH, Zurich Report, 1977.
(7) Larson, A. C.; von Dreele, R. B. *Generalized Structure Analysis System, GSAS*; (Los Alamos National Laboratory Report LAUR 86–748, 1986.
(8) Wiles, D. B.; Young, R. A. *J. Appl. Cryst.* **1981**, *14*, 149–151.

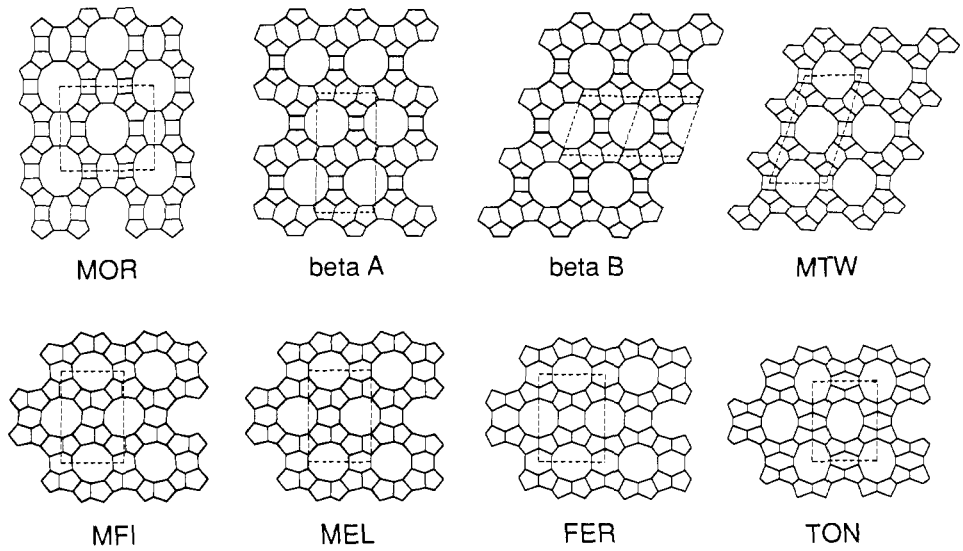

Figure 2. Projections along principal crystallographic directions of 8 distinct zeolite framework structures that contain 5-rings. The structures are drawn as straight lines connecting adjacent T-sites, with unit cell outlines dashed. In each of these cases, the framework appears in projection as a 3-connected net.

least-squares crystallographic methods can be used to refine the approximate model. The present approach to this structure solution problem relies on quantitation of the chemical/geometrical constraints that zeolite structures are known to obey. The method automatically determines ways in which the required number of T-atoms can, subject to the defined space group symmetry, be placed within the unit cell so as to generate viable zeolite models; viability is determined based on the degree to which the model matches the defined chemical and geometrical constraints. The method seeks to determine all of the viable structures. The appropriate framework for the material in question is then selected from the set of viable structures produced based, for example, on the model pore characteristics and on the degree to which the simulated powder diffraction pattern matches that observed experimentally. The effectiveness of the method can in fact be improved substantially by using the degree to which the model matches a target powder diffraction pattern as an additional constraint within the structure development process. In principle, additional constraint terms could also be added when more specific information about a particular structure is known.

2.3. The Zeolite Figure of Merit. Given the known (or assumed) unit cell dimensions, symmetry, and the number of T-atoms per unit cell, n_T, we construct a figure of merit that quantifies the reasonableness of a given arrangement of the unique T-atoms in the unit cell. We use this figure of merit as the basis for adjusting the unique T-atom arrangement so as to most closely match the required structural characteristics.

The zeolite figure of merit, H, is defined as

$$H = \alpha_{T\text{-}T}H_{T\text{-}T} + \alpha_{T\text{-}T\text{-}T}H_{T\text{-}T\text{-}T} + \alpha_{\langle T\text{-}T\text{-}T\rangle}H_{\langle T\text{-}T\text{-}T\rangle} + \alpha_{coordination}H_{coordination} + \alpha_{projection}H_{projection} + \alpha_{merge}H_{merge} + \alpha_{pore}H_{pore} + \alpha_{PXD}H_{PXD} + \alpha_{PND}H_{PND}$$

where H_x's are the various contributors and α_x's are the corresponding weights used in forming the total figure of merit. The weight assigned to each term has been adjusted so as to optimize the practical success of the method; it is generally unnecessary to alter these weights from the values specified below. By definition, the lower the value of the total figure of merit, the more physically reasonable the model structure. This figure of merit can be applied to any set of T-atom positions within a unit cell, whether or not it resembles a zeolite. It is, in fact, initially applied to *random* positions. By adjusting an initial, random set of unique T-atom positions so as to minimize the figure of merit, we produce viable structures that have the defined unit cell dimensions and symmetry.

It should be stressed that this figure of merit provides a quantitative measure of how well a given arrangement of the n_T T-atoms in a unit cell of *the prescribed dimensions and symmetry* satisfies the defined constraints. Minimizing this figure of merit is not equivalent to minimizing a thermodynamic energy. No oxygen atoms are included in the model, nor is there any explicit accounting for the framework or nonframework composition. The structure with the lowest figure of merit is, in general, unlikely to be the most thermodynamically stable arrangement of the atoms defining the known composition. These types of crystalline microporous solids crystallize under kinetic control, usually as metastable products. The more thermodynamically stable structures that form under the synthesis conditions are almost invariably more condensed and, therefore, of substantially less interest. The present procedure can, of course, also be used to determine these more condensed structures, if 4-connected, provided that the appropriate unit cell dimensions and symmetry are prescribed.

The first five components of the figure of merit are definable for each T-atom in a proposed structure, whereas the last four are definable only on the basis of a complete collection of atoms within a unit cell. The distance, angle and average angle terms are derived from the geometries observed in known zeolite structures. Histograms of T–T distances, T–T–T angles, and average T–T–T angles about one T-atom taken from structure determinations of 32 representative zeolite frameworks[9] are displayed in Figure 3. The simulated annealing optimization process, discussed further below, is defined so as to reproduce Boltzmann statistics. Potential energy curves are thus defined which, interpreted in the Boltzmann sense of probabilities being proportional to $\exp(-E/k_BT)$, reproduce the histograms of Figure 3; continuous curves are actually fitted to the discrete curves predicted by this Boltzmann interpretation of the histograms. These smoothing spline fits[10] are shown in Figure 4. These forms of the first three terms in the zeolite figure of merit are used in all the work described subsequently. Note that only at one given temperature would the energy curves of Figure 4 generate the histograms of Figure 3. The temperature actually chosen corresponds to one reached late in the stages of annealing (see below).

The coordination term, $H_{coordination}$, accounts for the four-connectedness of zeolite frameworks. The neighborhood of each T-atom is inspected to determine which T-atoms are linked to it, that is, those that are at less than a defined cutoff distance (typically 5.0 Å). These linkages determine, based on the associated distances and angles, the contributions from Figures 3 and

(9) Newsam, J. M.; Treacy, M. M. J. *Zeolites*, in press.
(10) Lancaster, P.; Salkauskas, K. *Curve and Surface Fitting: An Introduction*; Academic Press: London, 1986.

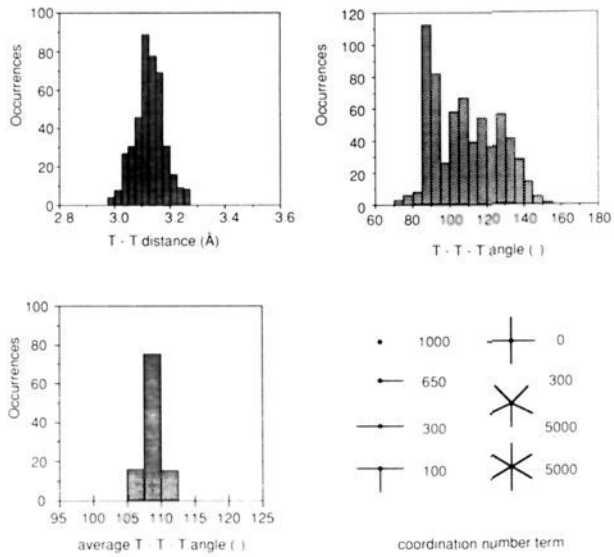

Figure 3. Histograms of individual T–T distances (upper left), T–T–T angles (upper right) and average T–T–T angles (bottom left) for 32 representative zeolite frameworks. The contributions of the various T-atom coordination numbers to the energy are illustrated at the bottom right.

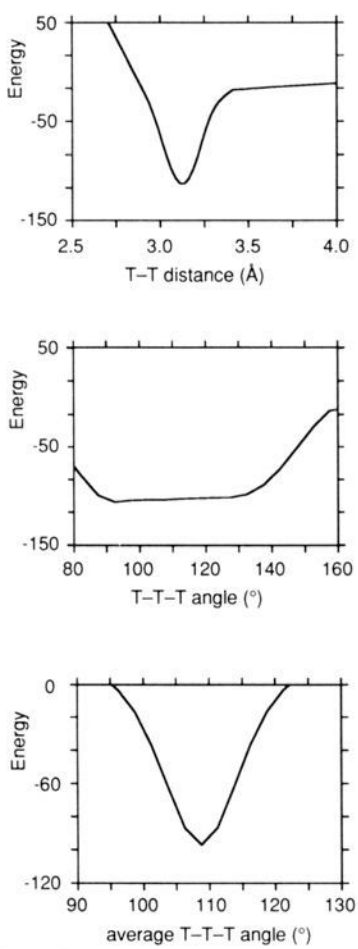

Figure 4. Smoothing spline fits to Boltzmann interpretations of the histogram data in Figure 3. These are the forms of the potential curves actually used in the simulated annealing procedure.

4. In addition, the coordination number term provides bias in favor of the desired coordination number(s) by adding a repulsive contribution to the energy for coordination numbers that are not desired. Typically, for zeolite systems, values of 1000, 650, 300, 100, 0, 300, and 5000 are used for coordinations of 0, 1, 2, 3, 4, and 5 or more (Figure 3). The correspondence between coordination number and repulsive energy needs to be adjusted appropriately for other coordination environments, such as in the interrupted frameworks in which some T-atoms are only 3-connected, or in framework structures containing both tetrahedrally- and octahedrally-coordinated framework cations. The implementation of the present method has been structured to accommodate, if necessary, separate definition of the preferred coordination number and of the other geometrical energy functions for each of the unique T-atoms.

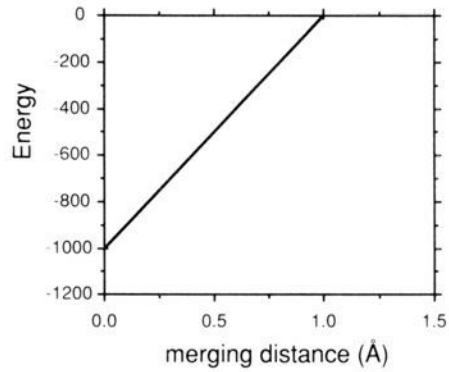

Figure 5. The contribution to the energy based on the merging of two symmetry-related T-atoms. Merging is permitted only when the two atoms are at less than a defined minimum distance, typically 1 Å.

The projection term exploits the observation that the projections of zeolite frameworks along one or more crystallographic direction typically appear as 3-connected nets (Figure 2). This property allowed the present simulated annealing method to be explored initially for the simpler case of structures in projection.[2] Three linkages, rather than four, are seen in projection if either one of the four tetrahedral bonds or the vector from any two of the four T-atoms linked to the central one is parallel to the projection axis (Figure 2). The projection term then provides a negative contribution to the energy that scales as the square of the angle between the bond or vector and the projection axis. The vector or bonding direction is taken to be that already closest to parallel with the projection axis.

The merging term facilitates the handling of T-atoms that must lie on symmetry elements (termed special positions), a common occurrence in zeolite structures. The total number of atoms per unit cell, n_T, is equal to the product of the number of crystallographically unique atoms, n_{unique}, and the number of symmetry operators, n_{symm}, only when all T-atoms occupy general positions; the coordinates of crystallographically unique T-atoms alone are the independent variables. Consider, for example, the case of a crystallographically unique T-atom approaching a mirror plane. By definition, the T-atom related by the mirror operation also approaches the mirror plane; the parent and the mirror-related T-atom occupy the same position in space when the unique T-atom actually reaches the mirror plane and the total number of distinct T-atoms in the unit cell generated from this parent is halved. To facilitate this placement of one or more of the unique T-atoms on a special position, the unique T-atom and the symmetrically related T-atom are defined to have merged at some point before exact overlap is achieved. Typically, when this merging is allowed, symmetry-related atoms that become closer than 1 Å are converted into one atom (at the unadjusted coordinates of the unique atom), and H_{merge} is given a negative contribution according to Figure 5. Such merging is permitted while the total number of atoms within the unit cell remains equal to or greater than n_T. This merging term therefore requires definition of the number of unique T-atoms, n_{unique}, as an input parameter. While n_T can be measured, n_{unique} must often be assumed based on the basis of the known number of symmetry operations and value of n_T. It is usually necessary to try several values of n_{unique}. Experimental data on the value of n_{unique}, such as from ^{29}Si or, where appropriate, ^{27}Al or ^{31}P NMR[11] could therefore be helpful in facilitating structure

solution. In certain space groups there is only one set of special positions, allowing one coordinate or coordinate interrelationship to be fixed. Such site constraints can also be used to facilitate the search for viable structural models.

Both sorption and catalytic data for a zeolite can indicate the approximate size of the apertures in the framework and, hence, the number of T-atoms in the rings defining them. Additionally, compositional and infrared data can suggest the presence of certain smaller rings such as 4-, 5-, or 6-rings. Exact computation of the number of T-atoms defining the larger rings that are present in a trial structure (by, for example, constructing a Voronoi diagram[12]) is unfortunately computationally expensive. As a simpler means of favoring those models with pores of approximately the desired dimensions a term, H_{pore}, is introduced into the figure of merit. This term is associated with 1, 2, or 3 cylinders or spheres that are placed in the unit cell and considered part of the structure, along with the T-atoms. The cylinder axis is defined parallel to a crystallographic direction, and the radii of sphere(s) or cylinder(s) are input parameters. These "objects" are repulsive potentials, Gaussian about their centers, the coordinates of which are treated as variables to be optimized in the annealing.

As discussed further below, the geometrical constraints described above can be satisfied by large numbers of possible structures in low symmetry cases. To improve the discrimination toward the structure that is correct for the particular material in question, the figure of merit can include contributions based on the degree of match between powder X-ray or neutron diffraction data computed on the basis of the model and that measured. The experimental powder diffraction data are input as a series of integrated intensities with associated Miller indices, weights, and multiplicities. For powder data such a list will, in general, include groups of reflections for which overlap prevents separate intensity estimations and which must therefore be treated as a combined intensity sum. The calculated powder diffraction pattern is first scaled to have identical total intensity to that observed, and H_{PXD} (or H_{PND}) is then defined as the weighted sum of the squares of the differences between the observed and calculated intensities. Inclusion of both X-ray and neutron powder diffraction data in the simulations increases the CPU time required for a simulation by about a factor of 4. The information content of the diffraction data is sufficiently high that even an approximate simulation is valuable. For the zeolite test cases described below, for example, it proved unnecessary to include the oxygen atoms in the PXD simulations.

The weights associated with each separate term included in the full figure of merit are typically set to unity, save for the values $\alpha_{T\text{-}T\text{-}T} = 3.0$ and $\alpha_{\langle T\text{-}T\text{-}T\rangle} = 6.0$. The weights can be adjusted if necessary to facilitate convergence in particular cases. In practice, for problems that require more than one pair of symmetry-related atoms to merge α_{merge} is usually set to 2.5. In the present applications of this solution method to known structures, we have varied only α_{merge} and α_{PXD} (see below).

2.4. Some Technical Details of the Zeolite Figure of Merit Calculation. The model generation procedure takes as input data the space group symmetry and, by definition, all the generated models have that symmetry. It is therefore important that the correct symmetry be determined, or that each of the possible symmetries be adequately considered. As the subsequent examples illustrate, some success is achieved on assuming a symmetry that is a subgroup of the maximal space group symmetry for the framework. However, the "complexity" of the minimization problem is defined by the number of unique T-atoms for which positions must be defined, making solution substantially more taxing in such subgroup cases. The importance of the correctness of the symmetry information makes it prudent also to check that the input symmetry operators form a mathematical group (by possessing a multiplicative identity, a multiplicative inverse for each element, closure under multiplication, and associativity under multiplication).

Computation of the coordination, distance and angle terms in the zeolite figure of merit requires determining those T-atoms that are within a spherical shell of the central T-atom which, calculated simply, would be $O(n_T^2)$ in complexity. Using a grid search reduces the complexity to $O(n_T)$.[12] For these and the merging contributions to the figure of merit, only the energy associated with crystallographically unique T-atoms must be calculated, as the value of such terms for the crystallographically equivalent atoms is identical. Information associated with the merging of atoms at a unique T-atom site must be propagated to symmetry-equivalent sites. The propagation of the merging is most easily accomplished using the group multiplication table of the symmetry group. A unique atom is defined as the atom generated by the identity operation. If the atom generated by operation S_i is then merged with the unique atom, the atom generated by S_j is merged with the atom generated by S_jS_i. The value of $S_k = S_jS_i$ is provided by the group multiplication table.

2.5. Simulated Annealing Applied to the Zeolite Figure of Merit. The figure of merit described in detail above provides a quantitative measure of how close a given arrangement of T-atoms in the known unit cell is to being a viable model for a zeolite structure. We now need a method of adjusting the T-atom coordinates so as to produce the most reasonable models, those that have the lowest values of the figure of merit, or "energy". This optimization is achieved by simulated annealing,[13-16] a proven algorithm for minimizing multidimensional functions. Starting at a point in the multidimensional space with calculated energy E_{old}, another point is generated by perturbing the original point. The new point is accepted if its energy, E_{new}, is less than or equal to E_{old} or if the energy difference $\Delta E = (E_{new} - E_{old})$ is positive, with a specified transition probability that depends on ΔE and a temperature, T.[17] In practice, the new configuration is accepted if $\exp(-\Delta E/T)$ is greater than a random number picked between 0 and 1. In the simulated annealing procedure,[13-16,18] the simulation is commenced at high temperature where most attempted moves are accepted and the temperature is then slowly reduced. The transition probability is reduced in consort so that the average energy of the sampled points in the space also diminishes. At the conclusion of the annealing, the resulting point will in general be near the global energy minimum for the system.

In the present case of zeolite frameworks, the multidimensional space is the space of the positions of the n_{unique} unique T-atoms within the unit cell, the initial point in this space is a set of random positions for these unique T-atoms, and the perturbation step adjusts their coordinates. The transition probability must be such that equilibrium statistics are reached.[16] In addition, the transitions, and hence the annealing schedule, must be such that regions of the parameter space are not kinetically excluded from examination.

Appendix I in the supplementary material lists C pseudo-code for the present implementation of the simulated annealing scheme. Typical values for the temperature-decrement factors, $T_{fact_n}(T)$, are 0.8 throughout the annealing, although the temperature decrement can be scaled according to the evolution with temperature of the system's specific heat (Figure 6). The perturbation step is carried out by the jiggle routine, which moves a T-atom in a random direction by a random amount within a sphere in crystallographic coordinates. The size of this sphere is arranged to decrease with temperature, typically starting at 1.4 Å and ending

(11) Engelhardt, G.; Michel, D. *High-Resolution Solid-State NMR of Silicates and Zeolites*; John Wiley: New York, 1987.
(12) Sedgewick, R. *Algorithms*, 2nd ed.; Addison-Wesley: Reading, MA, 1988.
(13) Kirkpatrick, S.; Gelatt, C. D.; Vecchi, M. P. *Science* **1983**, *220*, 671-680.
(14) Kirkpatrick, S. *J. Stat. Phys.* **1984**, *34*, 975-986.
(15) Press, W. H.; Flannery, B. P.; Teukolsky, S. A.; Vetterling, W. T. *Numerical Recipes, The Art of Scientific Computing*; Cambridge University Press: Cambridge, 1986.
(16) Kalos, M. H.; Whitlock, P. A. *Monte Carlo Methods: Volume I—Basics*; Wiley-Interscience: New York, 1986.
(17) Metropolis, N.; Rosenbluth, A. W.; Rosenbluth, M. N.; Teller, A. H.; Teller, G. *J. Chem. Phys.* **1953**, *21*, 1087-1092.
(18) Pannetier, J.; Bassas-Alsina, J.; Rodriguez-Carvajal, J.; Caignaert, V. *Nature* **1990**, *346*, 343-345.

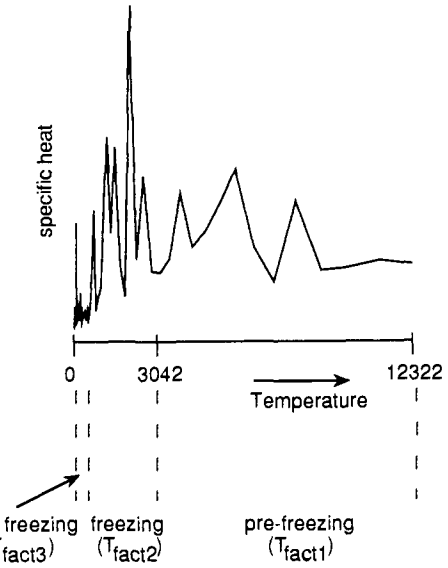

Figure 6. A plot of the change in the system specific heat, the variance of the system energy divided by the temperature, with temperature in a typical run of the simulated annealing procedure. The temperature decrement factor, T_{fact_n}, can be different for each of the three indicated regions of the annealing, generating the function $T_{fact}(T)$ used in Appendix 1.

at 0.1 Å for solely geometric optimization, and starting at 0.5 Å and ending at 0.01 Å when PXD or PND data are included to a resolution of d = 3 Å. The decrement is chosen to be either linear or quadratic in the temperature. The jiggle routine allows, as above, for specification of constraints on the coordinates of one or more of the unique T-atoms. The routine METROP(ΔE, T), defined by min{1, exp($-\Delta E/T$)}, is the standard Metropolis transition probability for Boltzmann statistics.[17] Throughout the annealing process, low-energy frameworks that are 4-connected are output so that the (single) structure produced at the finish of the annealing is not the only data gathered from one run.

2.6. Ancillary Tools. The present simulated annealing procedure has the capacity for generating large numbers of hypothetical framework structures, particularly when only geometrical constraints are imposed (see Table I). Only one of these hypothetical framework structures is likely to be correct for the particular material in question (although intergrowths of two or more structures are relatively common in zeolite systems; their presence is apparent in the measured powder X-ray diffraction pattern). Efficient use of this simulated annealing procedure thus requires having a means of collating the collective results of many runs as a set of unique topologies and of recognizing which of the several topologies produced in any one run have not been determined previously. The coordination sequences out to a defined shell from the central atoms[19] and, to a lesser extent, the Wells circuit symbols[20] can be used as characteristics of a zeolite framework topology. The coordination sequence is defined on the graph of the framework connectivity. For each crystallographically unique T-atom the kth entry in the coordination sequence is the number of nodes in the graph at a graph distance k from this T-atom, that is the number of T-atoms in its kth coordination shell. The connectivity graph is not periodic and is, in fact, infinite in extent. However, for unit cell volumes typical of most zeolites, if the coordination sequences out to k = 10 for two structures are identical, the probability that the topologies are also identical approaches one.

The set of n_{unique} coordination sequences for a given structure is then used here as the basis for determining whether two frameworks have identical topologies. A breadth-first search, which determines all the atoms in the first coordination shell, then those in the second, and so on, is used to compute the coordination sequences from the graph of the framework connectivity.[12] The coordination sequences for all the sets of T-atom positions output from an annealing run are computed and used to reduce the data to a unique set of topologies. Results from the full set of annealing runs, distinct only in initial pseudo-random number seed, are further collated to produce a single set of topologically unique results for a given set of input data. For the test results presented here, the actual set of coordination sequences for the known topology is then compared against this database of results to determine whether the actual structure has been "solved" by the simulated annealing procedure.

Knowledge of the coordination sequences for the "correct" structure is, of course, unavailable when the method is applied to an unknown structure. In such cases the screening of the full set of unique topologies involves firstly a visual inspection of the structures in projection along the three crystallographic directions (see Figures 7 and 8 below). Typically, at least 50% can be rejected based on, for example, being 2-dimensional sheet or 1-dimensional structures, having an absence of suitable pore structure, or, more difficult to quantify, lacking the visual symmetry typical of most known zeolite structures. Those structures passed by this first screening are then optimized further by conventional distance least squares[5,6] and the PXD pattern computed[8,21] and compared against observation. These latter calculations can be performed near-automatically on a large number of structures by means of a procedure that introduces the required oxygen atom positions, determines the necessary symmetry interrelationships, and then generates files in exactly the formats required by the DLS-76[6] and FINAX[21] crystallographic refinement programs.

3. Results

3.1. Solely Geometric Figure of Merit. A single run of the simulated annealing method, using only T–T distance, T–T–T angle, and average angle, coordination, and merging terms of the zeolite figure of merit, was made for 84 of the currently known zeolite structures, using the crystallographic data given for the representative structure in ZeoFile.[9] The unit cell dimensions and space group and values of n_T and n_{unique} are taken from those of the representative structure. The same parameters and weights in the zeolite figure of merit are used on all structures, except that α_{merge} is increased to 2.5 in those cases for which more than one atom merging is necessary. As above, a structure is considered solved if the coordination sequence for one of the final set of structures generated by the simulated annealing matches that of the representative structure of the known material.

The single first run gives the correct structure in 25 (30%) of the total of 84 cases (Table I). The structures that were obtained on the basis of the input data appropriate for the MON and VFI frameworks are shown in Figures 7 and 8. Of those structures not solved, those having six or fewer unique T-atoms[9] were selected for further runs, with only the initial pseudo-random number seed being changed between runs. The final results are listed in Tables I and II. The method is clearly successful, with 57 out of the 65 structures reproduced. In aggregate, the full set of calculations required to produce Table I consumed about a week of CPU time on a cluster of half-a-dozen 20-MHz SiliconGraphics Personal Irises.

3.2. Geometric and PXD Figure of Merit. An analogous set of calculations was performed using, in addition, a PXD diffraction term, H_{PXD}, in the zeolite figure of merit. As experimental PXD data for most of the materials for which structural data are known[9] are not available, synthetic data are used. The PXD patterns were calculated for $2\theta \leq 30°$ using the Cu Kα wavelength of 1.5418 Å from the known representative structures assuming, where possible, a chemical composition of SiO_2.[21] The maximum intensity in the calculated PXD pattern is scaled to 1000, and standard deviations of 1, 2, 3, and 4 are assigned to intensities greater than 0, 40, 80, and 120 in an effort to mimic approximately

(19) Meier, W. M.; Moeck, H. J. *J. Solid State Chem.* **1979**, *27*, 349.
(20) Wells, A. F. *Three Dimensional Nets and Polyhedra*; Wiley: New York, 1977.
(21) Hovestreydt, E. R. *J. Appl. Cryst.* **1983**, *16*, 651–653.

Table I. Zeolite Frameworks Solved by Geometric Optimization[a]

code	n_{max}	n_{unique}	n_{symm}	n_T	n_{found}	$n_{n=n_T}$	rank	n_{run}
ABW	1	2	4	8	7	7	4	1
AEL	3	6	8	40	125	17	1	62
AFG	3	3	24	48	97	61	2	30
AFI	1	2	12	24	3	3	1	1
AFY	2	4	6	16	129	11	1	90
ANA	1	1	96	48	4	4	1	1
APC	2	4	8	32	45	45	5	20
ATO	1	2	18	36	10	10	1	1
AlPO4-21	3	6	8	48	202	202	113	130
ATN	1	2	8	16	6	6	1	1
ATT	2	6	4	24	11	11	2	20
ATV	2	2	16	24	17	15	1	1
AWW	2	4	16	48	563	8	7	150
BIK	2	6	1	6	38	38	4	20
BRE	4	4	4	16	93	93	14	70
CAN	1	2	6	12	2	2	1	1
CAS	3	3	8	24	5	5	2	1
CHA	1	1	12	12	2	2	1	1
DAC	4	4	8	24	467	76	15	70
DOH	4	4	24	34	223	43	21	70
EAB	2	2	24	36	10	9	3	1
EDI	2	3	4	10	2	2	1	1
EMT	4	4	24	96	22	22	2	20
EPI	3	3	8	24	9	9	7	1
ERI	2	2	24	36	55	45	3	30
FAU	1	2	96	192	2	2	2	1
FER	4	4	16	36	83	18	5	20
GIS	1	4	4	16	31	31	27	54
GME	1	1	24	24	2	2	1	1
JBW	2	6	4	24	84	84	20	70
KFI	1	1	96	96	2	2	2	1
LAU	3	6	4	24	47	47	9	70
LEV	2	2	36	54	17	8	2	2
LIO	4	4	12	36	72	55	2	20
LOS	2	2	24	24	6	5	1	1
LTA	1	2	192	192	68	9	2	23
LTL	2	2	24	36	29	25	4	3
MAZ	2	2	24	36	9	6	1	1
MEI	4	4	12	34	93	2	1	70
MEP	3	3	48	46	10	2	1	1
MER	1	2	16	32	5	5	1	1
MON	1	1	32	16	5	4	1	1
MOR	4	6	8	48	78	78	6	130
MTN	3	3	96	136	106	6	1	23
NAT	2	3	16	40	16	4	3	9
NON	5	5	32	88	437	139	3	90
OFF	2	2	12	18	6	4	1	1
-PAR	4	4	8	32	209	111	16	100
PHI	2	4	4	16	1	1	1	1
α-quartz	1	1	6	3	1	1	1	1
RHO	1	1	96	48	6	5	2	1
-ROG	3	3	32	48	600	51	20	100
SGT	4	4	32	64	120	6	1	20
SOD	1	2	24	12	112	7	4	30
STI	4	5	8	36	127	35	15	90
TON	4	4	8	24	62	26	1	20
VFI	2	2	24	36	6	2	1	1
-WEN	3	3	12	20	466	10	5	100

[a] The number of crystallographically distinct T-atoms in the maximal symmetry setting for each framework is listed as n_{max}, whereas n_{unique} is the number of crystallographically distinct T-atoms in the symmetry of the representative crystal structure given in ZeoFile[9] taken as the basis for the present simulations. The order of the corresponding space group, that is the number of symmetry operators, is n_{symm}. The total number of T-atoms in the unit cell is n_T. The total number of topologically distinct hypothetical structures found is listed as n_{found}, and the number that have the correct value of n_T is listed as $n_{n=n_T}$. The position of the actual structure in the list of hypothetical results is listed as rank, with unity indicating that the actual structure had the lowest value of the zeolite figure of merit. Finally, n_{run} indicates the number of times the algorithm was run for the same set of input data appropriate for the given structure, but with differing initial pseudorandom number seeds.

the uncertainties expected in the experimental data. The PXD pattern measured from a real material will, of course, reflect the scattering from the full unit cell contents, both framework species, non-framework cations, and sorbates or occluded template molecules. However, unless a substantial proportion of heavy elements are present in well-localized positions, the general distribution of intensities will be a reasonable discriminator for possible framework models. Using data carefully measured from real materials we would expect a degree of success similar to that obtained with the synthetic data. Only the PXD diffraction term, H_{PXD}, has been used here, but this could be supplemented or replaced by the neutron powder diffraction term, H_{PND}, if there were some significant question about the reliability of the PXD pattern alone.

In using H_{PXD} in the figure of merit, it has proved sufficient, in fact, to perform the calculation of the powder X-ray diffraction intensities in each Monte Carlo step in the simulated annealing based only on the T-atom (assumed Si) positions. Indeed, for some structures, the agreement between simulated and synthetic PXD data is better with oxygen atoms completely absent than with oxygen atoms included at the midpoints of the T–T vectors. The

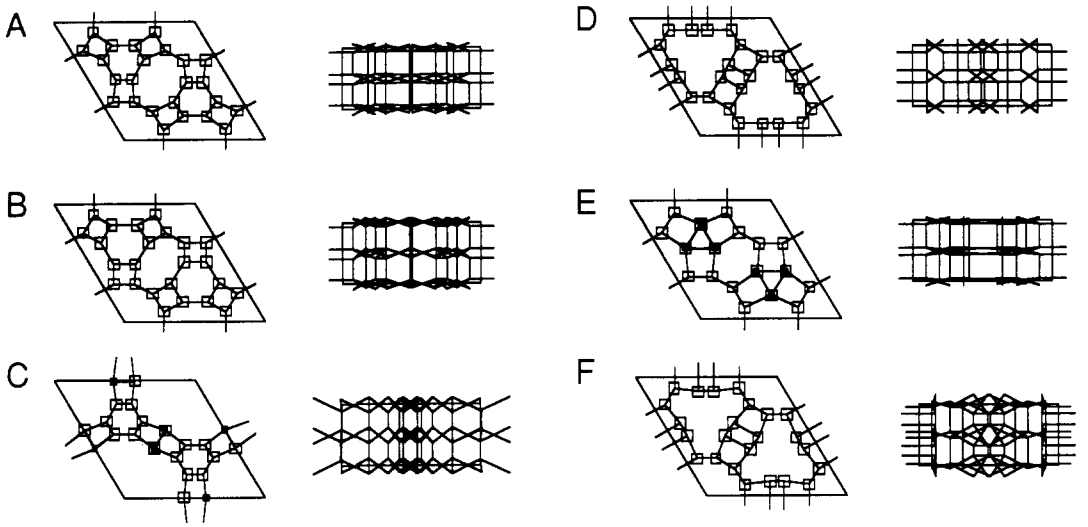

Figure 7. The six distinct 4-connected frameworks produced in the single run using data appropriate for the VFI framework drawn as [001] (left) and [100] projections (see Table I). The computed energies of the six structures are −4907 (A), −4939 (B), −3891 (C, the observed structure type), −1518 (D), −1459 (E), and −3307 (F). Only C and E have the required number of T-atoms, $n_T = 36$. The other four structures have $n_T = 48$.

Table II. Zeolite Frameworks Not Solved by Geometric Optimization[a]

code	n_{max}	n_{unique}	n_{symm}	n_T	n_{found}	$n_{n=n_T}$	n_{run}
AEI	3	6	8	48	21	21	90
AFT	3	6	12	72	12	12	90
*BEA	9	9	8	64	9	0	96
beta B	9	9	8	64	14	0	99
BOG	6	6	16	96	63	63	90
BPH	3	6	6	28	89	11	130
HEU	5	5	8	36	155	70	90
THO	3	6	8	40	107	1	200

[a] Legend is the same as for Table I. Other known zeolite structures not included in Tables I and II are AET ($n_{max} = 5$; $n_{unique} = 10$ for the representative structure given in ZeoFile[9]), AFO (4; 8), AFS (3; 12), APD (2; 8), AST (2; 4), -CHI (4; 7), DDR (7; 7), EUO (10; 10), GOO (5; 8), LOV (3; 9), LTN (4; 8), MEL (7; 7), MFI (12; 12), MFS (8; 8), MTT (7; 7), MTW (7; 7), PAU (8; 8), -STO (12; 12), and YUG (2; 8).

results of these simulations are given in Tables III and IV in the supplementary material. Of the 61 structures on which the method was applied, 59 are successfully reproduced. In all but two cases, the structure found with the lowest energy is the known structure. The PXD and merging weights have been adjusted for several of these results, but otherwise the parameters are identical for all the structures. Tables III and IV represent much smaller numbers of runs than do Tables I and II, but because of the more compute-intensive nature of the simulations with H_{PXD} included, an equivalent amount of CPU time is required.

4. Discussion

4.1. Geometric Figure of Merit. The geometric considerations defined above are quite successful in allowing the structure of zeolites and related materials to be predicted on the basis of information that is, in principle, easily determined experimentally. For many of the known cases, the actual structure as produced by this simulated annealing method ranks among the lowest of all of the hypothetical structures produced for the given unit cell size, symmetry, and values of n_T and n_{unique}. Nevertheless, for most of the cases listed in Tables I and II, many hypothetical structures are generated in addition to the known structure (Figures 7 and 8). This suggests that it may be possible to improve still further the geometric figure of merit so as to capture whatever other features distinguish those structures that are produced by current synthesis methods from those that remain merely hypothetical. It also suggests, given the reasonableness by the present terms of many of the hypothetical structures, that a much larger range of materials might be made.

The simulated annealing method is a rapid generator of hypothetical 4-connected framework structures. The more than 5000 hypothetical structures noted in Tables I and II should be compared with the approximately 1000 hypothetical structures that, in aggregate over the past 5 decades, have been documented by zeolite researchers using classical physical model building.[22] Many of the generated hypothetical structures are interesting, either from a topological perspective, or as possible models for yet to be synthesized materials. However, no attempt to categorize this rapidly growing database of hypothetical structures has yet been made.

For a large number of the 84 known zeolite structures noted in Tables I and II the value of n_{unique} for the representative structure taken from ZeoFile[9] is larger than the number of crystallographically distinct T-atoms in the maximal symmetry setting for the framework, n_{max}. For example, for all of the aluminophosphates, Al–P alternation dictates that $n_{unique} \geq 2n_{max}$. The key parameter in determining the success of the simulated annealing approach is the value of n_{unique}. For those cases in which $n_{unique} \geq 5$, recognition of a higher, or even maximal, symmetry setting based on the supergroups of the space group determined for the material in question may then greatly facilitate determining the correct framework model. Subsequent least-squares optimizations could then be made in the actual space group setting. For example, one of the failures listed in Table II is the BPH framework, the type of material for which, Beryllophosphate-H, has strict Be–P alternation, space group $P321$, and $n_{unique} = 6$. If the higher symmetry setting that might be appropriate for an SiO_2 composition of $P\bar{6}2m$ is used, n_{unique} becomes three, and the structure proves straightforward to reproduce.

4.2. Geometric and PXD Figure of Merit. The most obvious approach to reducing the number of hypothetical results produced by the present simulated annealing method is to include the experimentally measured PXD in the zeolite figure of merit. As is clear from Tables III and IV (supplementary material), such information is very effective at increasing the robustness of the method. That is, if the method produces an answer with PXD information considered, that answer is probably correct. It is to

(22) Smith, J. V. *Chem. Rev.* **1988**, *88*, 149–182.

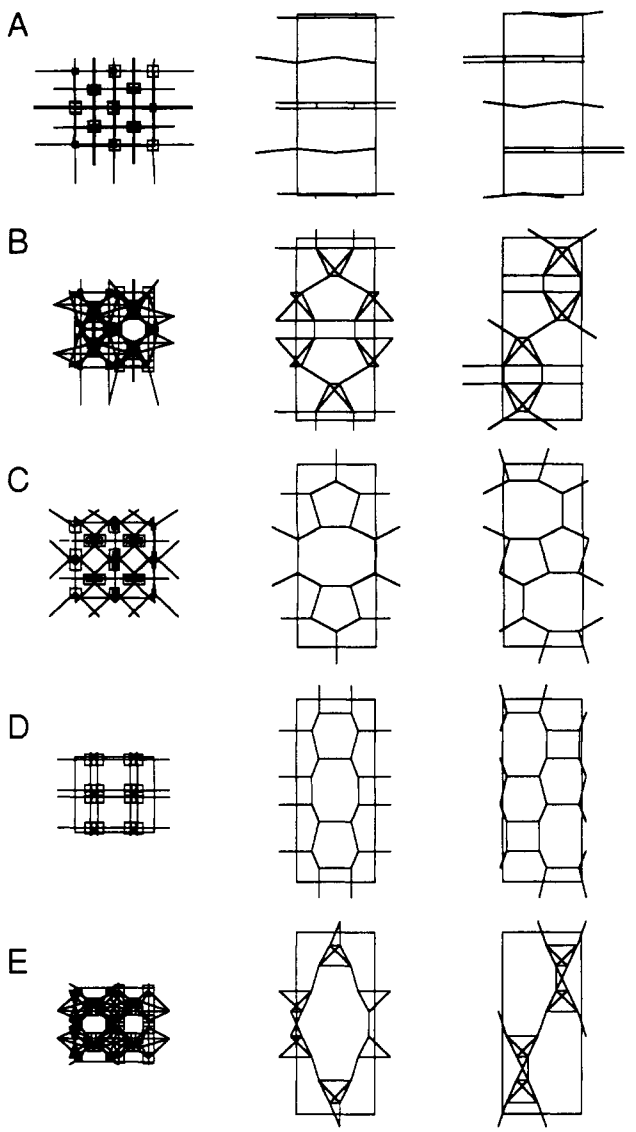

Figure 8. The five distinct 4-connected frameworks produced in the single run using data appropriate for the MON framework as input drawn as [001], [100], and [010] projections (see Table I). The computed energies of the five structures are −2187 (A), −1947 (B), −3343 (C, the observed structure type), −1958 (D) and −308 (E).

be expected, as above, that the method would be similarly successful were real experimental data to be used in place of the synthetic PXD data used here. It is noteworthy that to reproduce the synthetic PXD data to the level of approximation needed to be useful as a model discriminator the addition of oxygen atoms to the T-atom model was unnecessary.

On a small number of occasions, structures were found that gave reasonable values for the zeolite figure of merit with H_{PXD} included but were, in fact, not the correct structure. The likelihood of such false positive indications would, we anticipate, be reduced still further by increasing the range of the diffraction data beyond $2\theta = 30°$.

The PXD pattern is in a large number of cases a sufficient characterization of the experimental sample that the degree of match between observed and simulated patterns, combined *only* with the atom merging term, $H_{merging}$, allows the correct structure to be derived. Test attempts at solution of the same set of known zeolite structures gave successful results in 52 cases (Table V, supplementary material) and failures in 8 (Table VI, supplementary material). The measure of success is again taken to be reproduction of the set of coordination sequences for the known structure. This measure requires that the optimized T-atom coordinates be sufficiently accurate that the appropriate connectivity can be determined on the basis of proximities. Given that the T-atom positions are determined solely by $H_{merging}$ and H_{PXD} this criterion for success is quite demanding. This simplified use of the figure of merit involves, of course, no term that is zeolite-specific, and the results in Table V (supplementary material) thus demonstrate that the method can be applied *generally* to crystal structure solutions.

4.3. Notes for Structure Solution. Most zeolite structures can likely be solved by the present simulated annealing method based on purely geometric considerations if enough attempts are made based on the appropriate unit cell dimensions, symmetry, and values of n_T and n_{unique}. Clearly, if these data are not known unambiguously, sufficient attempts must be made with each of the possible combinations of values. In principle, one of the advantages of the present simulated annealing route to initial model derivation is that it is unbiased and not influenced by any incorrect "intuition" that accumulates from familiarity with known structures. For example, in attempting to solve the structure of ZSM-18 based on the diffraction and sorption data given in the original patent,[23] we considered a value $n_T = 34$ "unlikely" and ran simulations based only on $n_T = 32$ and 36. Following a description of the MEI framework of ZSM-18[24] and using the correct input of $n_T = 34$ (and $n_{unique} = 4$) the structure was "solved" quite readily (Table I and Table III, supplementary material).

4.4. Generalization of the Geometrical Functions Beyond Zeolites. Three of the structures listed in Table I, -PAR, -ROG, and -WEN, have interrupted frameworks, with one of the unique T-atoms linked to only three neighboring T-atoms. The remaining linkage is terminated in these structures as a hydroxyl function. The present approach is successful in reproducing these structures, given input data defining one of the unique T-atoms to be 3-connected. In these 3-connected structures, the specification of unit cell size, space group symmetry, and values of n_T and n_{unique} is apparently less constraining than for 4-connected structures, as very many hypothetical structures were produced in the runs for these three structure types (Table I), with the number of hypothetical structures arbitrarily limited to 600 in the case of -ROG.

In these cases, the geometry of the T-atom connectivity is altered only subtly by the presence of the single 3-connected T-atom, and the energy functions (Figures 3 and 4) were used without change. Extension to other types of coordinations is also relatively straightforward. For example, by merely shifting the entire energy vs T–T distance curve (Figure 4) by 0.3 Å to larger distances, shifting one energy vs T–T–T angle curve so that it is centered on 90° rather than 109.5° (together with an approximately 5° compression in the curve width), and specifying that one of the $n_{unique} = 2$ T-atoms should be 4-connected and the other 6-connected, the structure of malayaite, a mixed tetrahedral–octahedral stannosilicate[25] was reproduced in a first attempt in which neither H_{PXD} nor H_{PND} were included.

5. Conclusions

Direct, real-space solution of zeolite framework crystal structures by simulated annealing is plainly a viable alternative to conventional powder diffraction or model-building methods, at least for those structures that have fewer than ~6 crystallographically unique T-sites. Once the unit cell dimensions, symmetry, and the framework density are defined, the reasonableness of an arbitrary arrangement of the required number of T-atoms can be quantified on the basis of the established geometrical characteristics of zeolite structures. Simulated annealing is used to optimize the T-atom configuration based on these constraints. The solutions of the known zeolite structure types attempted by this method demonstrate a substantial success based on a single program pass. A nearly 90% success rate in reproducing those known structures with 6 or fewer unique T-atoms is achieved with persistence. Large numbers of hypothetical 4-connected framework structures are also generated, although the actual structures

(23) Ciric, J. U.S. Patent No. 3,950,496, 1976.
(24) Lawton, S.; Rohrbaugh, W. J. *Science* **1990**, *247*, 1319–1322.
(25) Higgins, J. B.; Ross, F. K. *Cryst. Struct. Comm.* **1977**, *6*, 179–182.

generally rank among those with the lowest value of the figure of merit. When a contribution to the figure of merit based on the degree to which the model matches a target powder diffraction pattern is included, the success and the robustness of the method are significantly improved. Using solely powder X-ray diffraction and framework density information proves sufficient, in fact, to reproduce a majority of the known zeolite frameworks. The geometrical terms can be adjusted straightforwardly for other classes of structures. The terms based on the degree of match between observed and calculated diffraction data are intrinsically general, and this simulated annealing approach is therefore broadly applicable.

Acknowledgment. We thank R. Rajagopalan, M. M. J. Treacy, and B. P. Flannery for helpful discussions.

Supplementary Material Available: Tables giving the results for those known zeolite frameworks using both geometric and powder X-ray diffraction pattern matching contributions to the zeolite figure of merit (Table III, structures reproduced; Table IV, structures not reproduced) and using only powder X-ray diffraction pattern matching contributions (Table V, structures reproduced; Table VI, structures not reproduced) and Appendix I, C pseudo-code for the simulated annealing procedure (5 pages). Ordering information is given on any current masthead page.

Fluctuations in Zeolite Aperture Dimensions Simulated by Crystal Dynamics

M. W. Deem,† J. M. Newsam,* and J. A. Creighton§

Contribution from Exxon Research and Engineering Company, Route 22 East, Annandale, New Jersey 08801, and BIOSYM Technologies Inc., 9685 Scranton Road, San Diego, California 92121-2777. *Received July 26, 1991*

Abstract: The lattice dynamics of zeolite frameworks have often been suggested to influence the performance of zeolite materials in catalytic and sorptive applications. In a direct study of the influence of the framework dynamics on pore structure, constant volume crystal dynamics methods are used to simulate variations in the aperture dimensions with temperature of the six representative zeolite structure types SOD (sodalite; 6-ring—six oxygen atoms define the aperture), RHO (rho; 8-ring), TON (theta-1; 10-ring), MFI (silicalite; 10-ring), LTL (Linde type L; 12-ring), and *BEA (beta; 12-ring). The framework flexibilities are explicitly modeled by a crystal mechanics force field with parameters taken from quantitative interpretations of Raman and infrared spectroscopic data. These simulations reveal substantial motion of the framework atoms about their equilibrium positions. The variations in the fluctuations of the effective aperture sizes with temperature depend on the framework connectivity, consistent with experimental observation. The frequency spectra of the O–O distances across the apertures reveal generally well defined periodicities in the pore window motion. The definition, extent, and period of the motion depend on the framework connectivity. It is most pronounced in the SOD and RHO frameworks, previously known from experiment to be most susceptible to static framework distortion. The change in cross-sectional area of the 12-ring window in the LTL framework with time is also periodic, a direct demonstration of pore-mouth breathing motion.

Introduction

The windows in zeolite crystal structures[1-3] dictate molecular sieving capabilities and control access to internal sites that are catalytically active or preferred for binding by sorbates. Effective dimensions calculated from crystallographic data, however, are substantially smaller than those deduced from molecular sieving properties.[1] It has long been speculated that this discrepancy reflects in part a thermally activated breathing motion of the zeolite pores.

The molecular sieving properties of a zeolite are readily measured by monitoring sorbate uptake gravimetrically.[1,4,5] When the kinetic diameter of the sorbate approaches that of the cross-sectional area of the largest zeolite apertures, the rate of uptake becomes slow, and the full sorption capacity is generally only achieved at elevated temperatures. Direct measurement of aperture dimensions as a function of temperature is, in principle, possible by diffraction, but the Debye–Waller factors for zeolite framework species derived from diffraction data usually compensate for a variety of other model deficiencies, including the effects of static disorder and inhomogeneity. Furthermore, the averaged diffraction results cannot indicate coupling of the dynamical motions of successive tetrahedra. Direct measurement of framework vibrations using spectroscopic techniques is possible, although it is only recently that proper lattice dynamical models for the complex structures of zeolites have been pursued. Crystal dynamics techniques have recently been applied to the motion of certain simple molecules within idealized zeolites,[6-13] and some

* Address correspondence to this author at BIOSYM Technologies Inc.
† Present address: Department of Chemical Engineering, University of California, Berkeley, CA 94720.
§ Present address: Chemical Laboratories, University of Kent, Canterbury CT2 7NH, England.

(1) Breck, D. W. *Zeolite Molecular Sieves: Structure, Chemistry and Use*; Wiley and Sons (reprinted by R. E. Krieger, Malabar FL, 1984): London, 1973.
(2) Barrer, R. M. *Hydrothermal Chemistry of Zeolites*; Academic Press: London, 1982.
(3) Newsam, J. M. *Science* **1986**, *231*, 1093–1099.
(4) Barrer, R. M. *Zeolites and Clay Minerals as Sorbents and Molecular Sieves*; Academic Press: London, 1978.
(5) Ruthven, D. M. *Principles of Adsorption and Adsorption Processes*; Wiley-Interscience: New York, 1984.
(6) Demontis, P.; Suffritti, G. B.; Alberti, A.; Quartieri, S.; Fois, E. S.; Gamba, A. *Gazz. Chim. Ital.* **1986**, *116*, 459–466.
(7) Demontis, P.; Suffritti, G. B.; Quartieri, S.; Fois, E. S.; Gamba, A. *Zeolites* **1987**, *7*, 522–527.
(8) Demontis, P.; Suffritti, G. B.; Quartieri, S.; Fois, E. S.; Gamba, A. In *Dynamics of Molecular Crystals*; Lascombe, J., Ed.; Elsevier: Amsterdam, 1987; Vol. 92, pp 699–704.
(9) Demontis, P.; Suffritti, G. B.; Quartieri, S.; Fois, E. S.; Gamba, A. *J. Phys. Chem.* **1988**, *92*, 867–871.
(10) Demontis, P.; Yashonath, S.; Klein, M. L. *J. Phys. Chem.* **1989**, *93*, 5016–5019.
(11) Yashonath, S.; Demontis, P.; Klein, M. L. *Chem. Phys. Lett.* **1988**, *153*, 551–556.
(12) Demontis, P.; Fois, E. S.; Suffritti, G. B.; Quartieri, S. *J. Phys. Chem.* **1990**, *94*, 4329–4334.

0002-7863/92/1514-7198$03.00/0